

The preparation of an arbitrary polarization-entangled mixed state of two photons with location decoherence

Chuanwei Zhang

Department of Physics, University of Texas at Austin, Austin, Texas 78712

We propose a scheme for preparing an arbitrary polarization-entangled mixed state starting from a pure state with location decoherence owing to the path difference. The scheme, using linear optical devices (beam splitter, half wave plate, quarter wave plate) and single-mode optical fibers, is feasible in experiment within current optical technology. We also give a simplified scheme for a special case $\rho = p |\psi\rangle\langle\psi| + (1-p) |\phi\rangle\langle\phi|$.

PACS numbers: 03.67.-a, 03.65.Ud, 42.25.Ja, 89.70.+c

Decoherence plays an important role in discussions of the foundations of quantum theory [1]. It typically arises as a result of the coupling between a quantum system and an unobserved environment, and then tracing out the environment, which yields the mixed state. This reduction of coherent superpositions into incoherent mixtures establishes a fundamental limit to quantum computation and communication [2]. The practical quantum information protocols therefore relies upon the understanding of the decoherence effects.

In the optical field, the “decoherence-free subspace” (DFS) [3], a special case of a two-qubit mixed state, has been demonstrated experimentally. DFS is important in quantum computation since it is immune to collective decoherence owing to its symmetry properties. In the experiment, the pure polarization-entangled state of two photons is produced using the process of spontaneous parametric down-conversion [4,5]. A controllable decoherence is then imposed on the state by passing the photons through the birefringent elements which couple the polarization modes with the frequency modes [3].

To study the entanglement concentration [6–8] and various applications [6,9,10] of mixed states requires the production of an arbitrary polarization-entangled mixed state of two photons. We approach this aim in this paper by coupling between the polarization modes and the location modes of the photons. The single-photon decoherence is then induced by separating the polarization modes (path differences) beyond the coherence length of the photon. In the scheme, beam splitters with variable polarization transmission coefficients (VBS) are used to obtain the location qubits and wave plates (half (HWP) and quarter (QWP)) control the polarizations. The path differences are adjusted by the single-mode optical fibers (SMOFs), which also unite different optical paths of a single photon into one [11]. The scheme is equivalent to a two-photon interferometer with single-photon one-order Mach-Zehnder (M-Z) interferometers in each path and therefore feasible within current optical technology.

Let us first specified the representation of an arbitrary two-qubit mixed state which guides our preparation

scheme. It is known that [12] for any two-qubit mixed state ρ there is an optimal pure-state ensemble with at most four states, and with all of them having the same entanglement of formation (EOF), i.e.

$$\rho = \sum_{k=1}^{\leq 4} p_k |\psi_k\rangle\langle\psi_k| \quad (1)$$

where $0 \leq p_i \leq 1$, $\sum_{k=1}^4 p_k = 1$, and $p_i \geq p_j$ for $i \leq j$. $|\psi_k\rangle$ are two-qubit pure states having the same EOF as ρ , that is, $|\psi_k\rangle$ are same up to some local unitary operations [13] and therefore $|\psi_k\rangle = U_k \otimes V_k |\Phi\rangle$, where U_k and V_k are local unitary operations and $|\Phi\rangle = \cos\theta |00\rangle + \sin\theta |11\rangle$ with $0 \leq \theta \leq \pi/4$.

Fig. 1

The experimental arrangement for our protocol is described by the schematic in Fig. 1. Spontaneous parametric down-conversion in two adjacent β -barium borate (BBO) crystals results in the initial polarization-entangled pure state $|\Phi\rangle$ [5], which is composed of two photon systems, A and B . The joint state of the system AB is described in the polarization basis $\{|HH\rangle, |HV\rangle, |VH\rangle, |VV\rangle\}$, where $|H\rangle$ and $|V\rangle$ are horizontal and vertical polarizations respectively. The VBSs η_i couple the polarization state $|\Phi\rangle$ with the location by transforming the location modes in the following way

$$|a\rangle_{initial} \rightarrow \sqrt{\eta_i} |a\rangle_{final} + \sqrt{1-\eta_i} |b\rangle_{final}, \quad (2)$$

where $|a\rangle$ and $|b\rangle$ are the location modes and $\sqrt{\eta_i}$ are the transmission coefficients of the VBSs.

Each photon has four optical paths $i_{A(B)}$ after three VBSs. In each path, the single-qubit polarization transformation (SPR) performs the local unitary operation on the polarization of each photon. The four paths $i_{A(B)}$ are then connected to a single-mode optical fiber (SMOF) at $G_{A(B)}$ by using four SMOFs. Denote $L_i^{A(B)}$ as the optical path lengths of path $i_{A(B)}$ from the BBO crystal to the points $G_{A(B)}$. If we choose the path lengths satisfying $L_i^A = L_i^B$ and $\Delta_{ij}^{A(B)} = |L_i^{A(B)} - L_j^{A(B)}| \gg \varrho_{coh}$ for different i and j , where ϱ_{coh} is the single-photon coherence

length, the polarization at each path will incoherently mix at $G_{A(B)}$. The locations are thus traced out and the decoherence effect results in the mixed state.

However, the mixed state still contains the information of the location since the photon from different path will arrive at the detector at different time. The polarization state space therefore is expanded by two discrete subspaces: two photons A, B arriving at the same time and at different time. If the time window of the coincidence counter is small enough so that only photons A, B from the same optical path length L_i^A and L_i^B contribute the coincidence counts, the polarization state of the photons are reduced to the subspace of the same arrival time. In this subspace, the state is just the two-qubit mixed state ρ since the detectors can not discriminate which path the photons are from if they arrive at the same time. The final SPR in each arm, along with PBS, enable analysis of the polarization corrections in any basis, allowing tomographic reconstruction of the density matrix [3,5,6].

The VBS can be implemented by using a one-order M-Z interferometer [8,14]. The $SPR_i^{A(B)}$ at the path $i_{A(B)}$, constructed with the wave plate sequences $\{\text{QWP}, \text{HWP}, \text{QWP}\}$ [8], perform the unitary operation U_i^A and V_i^B respectively. After the points $G_{A(B)}$, the photon loses its ability to interfere with itself, which yields the mixed state

$$\rho_0 = \sum_{i,j=1}^4 p_{ij} U_i \otimes V_j |\Phi\rangle\langle\Phi| U_i^\dagger \otimes V_j^\dagger. \quad (3)$$

where p_{ij} , determined by the transmission coefficients $\sqrt{\eta_i}$, is the combined probabilities with photons A and B on locations $|i\rangle_A, |j\rangle_B$ respectively. Denote T as the time window of the coincidence counter which satisfies $T < \Delta_{ij}/c$, where c is the velocity of the light. In this case, only photons from locations $|i\rangle_A |i\rangle_B$ are registered by the coincidence counter, which projects the reduced density matrix of the final state to

$$\rho = \frac{1}{F} \sum_{i=1}^4 p_{ii} |\psi_k\rangle\langle\psi_k| \quad (4)$$

where $F = \sum_{i=1}^4 p_{ii}$ is the normalized coefficient and also the successful probability of generating the mixed state ρ .

We must emphasize here that the post-selection by the detectors does not affect the using of ρ as a mixed state source. In fact, we only consider the quantum information processing in the subspace where two photons have the same arrival time. Such subspace is conservative and does not mix with other subspace. The detections only measure the final state in that subspace.

Obviously $p_{11} = \eta_1 \eta_2 \eta_3 \eta_5$, $p_{22} = \eta_1 \eta_2 (1 - \eta_3) (1 - \eta_5)$, $p_{33} = (1 - \eta_1) (1 - \eta_2) \eta_4 \eta_6$, and $p_{44} =$

$(1 - \eta_1) (1 - \eta_2) (1 - \eta_4) (1 - \eta_6)$. The remained problem is to maximize the final successful probability F under the restrictions $p_k = p_{ii}/F$. Since $p_1 \geq p_2 \geq p_3 \geq p_4$, $p_1 > 0$. Denoting $A_i = p_i/p_1$, the optimal values of F and η_i can be obtained by using Lagrangian Multipliers. The results are classified as

$$1. \quad A_i > 0 \text{ for } i = 2, 3, \quad \eta_1 = \eta_2 = (1 + \sqrt{A_2}) / \left(\sum_{i=1}^4 \sqrt{A_i} \right), \quad \eta_3 = \eta_5 = 1 / (1 + \sqrt{A_2}), \\ \eta_4 = \eta_6 = \sqrt{A_3} / (\sqrt{A_3} + \sqrt{A_4}), \quad \text{and} \quad F = \left(\sum_{i=1}^4 A_i \right) / \left(\sum_{i=1}^4 \sqrt{A_i} \right)^2.$$

$$2. \quad A_2 > 0, \quad A_3 = A_4 = 0, \quad \eta_1 = \eta_2 = \eta_4 = \eta_6 = 1, \quad \eta_3 = \eta_5 = 1 / (1 + \sqrt{A_2}), \quad \text{and} \quad F = (1 + A_2) / (1 + \sqrt{A_2})^2.$$

$$3. \quad A_2 = A_3 = A_4 = 0, \quad \eta_i = 1, \quad \text{and} \quad F = 1.$$

So far we have introduced a scheme for preparing an arbitrary polarization-entangled state of two photons using VBS and SMOF. However, we often meet a special set of mixed states with the form $\rho = p |\psi\rangle\langle\psi| + (1 - p) |\phi\rangle\langle\phi|$ in practical situation, where $0 \leq p \leq 1$ and $|\psi\rangle, |\phi\rangle$ are arbitrary two-qubit pure states. In this case, the scheme can be simplified. Assume $|\psi\rangle = U_1 \otimes V_1 |\Phi(\alpha)\rangle$, $|\phi\rangle = U_2 \otimes V_2 |\Phi(\beta)\rangle$ with $|\Phi(\theta)\rangle = (\cos\theta |HH\rangle + \sin\theta |VV\rangle)$, and $0 \leq \beta \leq \alpha \leq \pi/4$ for convenience. The initial state can be chosen as either $|\Phi(\alpha)\rangle$ or $|\Phi(\beta)\rangle$, which depends on the value of p to optimize the final successful probability.

Fig. 2

The experimental arrangement is described by the schematic in Fig. 2. The VBS and SMOF perform the same operations on the photons as those in Fig. 1. Entanglement transformation is performed on location $|1\rangle_A$ or $|2\rangle_A$ depending on which initial state is used ($|1\rangle_A$ corresponds to $|\Phi(\beta)\rangle$ and $|2\rangle_A$ to $|\Phi(\alpha)\rangle$). The distillation filters is used for entanglement transformation [6] and can be replaced with an one-order M-Z interferometer [8]. The decoherence process yields the final states for the different initial states $|\Phi(\beta)\rangle$ and $|\Phi(\alpha)\rangle$,

$$\rho = \frac{1}{P} (k_1 \eta_1 \eta_2 |\psi\rangle\langle\psi| + (1 - \eta_1) (1 - \eta_2) |\phi\rangle\langle\phi|) \quad (5)$$

$$\rho' = \frac{1}{P'} (\eta_1 \eta_2 |\psi\rangle\langle\psi| + k_2 (1 - \eta_1) (1 - \eta_2) |\phi\rangle\langle\phi|)$$

where $k_1 = \sin^2 \beta / \sin^2 \alpha$ ($k_2 = \cos^2 \alpha / \cos^2 \beta$) [15,8] is the maximally feasible transformation probability in experiment from $|\Phi(\beta)\rangle$ to $|\Phi(\alpha)\rangle$ ($|\Phi(\alpha)\rangle$ to $|\Phi(\beta)\rangle$). $P = k_1 \eta_1 \eta_2 + (1 - \eta_1) (1 - \eta_2)$ and $P' = \eta_1 \eta_2 + k_2 (1 - \eta_1) (1 - \eta_2)$ are the successful probability to obtain ρ and ρ' . The transmission coefficients $\sqrt{\eta_1}$ and $\sqrt{\eta_2}$ satisfy the restricted conditions $(1 - \eta_1) (1 - \eta_2) = A k_1 \eta_1 \eta_2$ for ρ and $k_2 (1 - \eta_1) (1 - \eta_2) = A \eta_1 \eta_2$ for ρ' , where $A = (1 - p) / p$. The optimization of P and P' yields that

$$P = k_1 (1 + A) / \left(1 + \sqrt{A k_1}\right)^2, \quad (6)$$

$$P' = k_2 (1 + A) / \left(\sqrt{k_2} + \sqrt{A}\right)^2,$$

with $\eta_1 = \eta_2 = 1 / (1 + \sqrt{A k_1})$ for ρ and $\eta_1 = \eta_2 = \sqrt{k_2} / (\sqrt{k_2} + \sqrt{A})$ for ρ' . Direct comparison between P and P' shows that when $0 \leq p \leq \frac{k_1(1-\sqrt{k_2})^2}{k_1(1-\sqrt{k_2})^2 + k_2(1-\sqrt{k_1})^2}$, $P' \leq P$ and $|\Phi(\beta)\rangle$ is used to obtain the maximally successful probability. Otherwise $P \leq P'$ and $|\Phi(\alpha)\rangle$ is used.

Fig. 3

In Fig. 3, the final successful probabilities P , P' and the transmission coefficient η_1 are plotted. Notice that if $\eta_{1(2)} = 0$, then $\eta_{2(1)} = 1$ and $P = P' = 0$, which means that only one optical path is selected and no mixed state ρ is produced. The probability P (P') reaches the maximal at certain η_1 , just as that predicted at Eqs. (6). A surprising thing is that there exist fixed points $(\eta_1, P) = (1 / (1 + k_1), k_1 / (1 + k_1))$ and $(\eta_1, P') = (k_2 / (1 + k_2), k_2 / (1 + k_2))$ for arbitrary parameter A . If the transmission coefficient η_1 is selected at those points, the final successful probabilities P , P' are constants, independent of the ratio of two components $|\psi\rangle$ and $|\phi\rangle$.

Fig. 4

Fig. 4 illustrates the optimal probability P , P' depending on the parameters A . As predicted by Eq. (6), $P \rightarrow k_1$, $P' \rightarrow 1$, for $A \rightarrow 0$, while $P \rightarrow 1$, $P' \rightarrow k_2$ for $A \rightarrow \infty$. These two cases correspond to that the final state ρ is approaching a pure state. There exist the minimum values of P (P') at $A = k_1(1/k_2)$. We may also notice that at certain value of A , $P = P'$, while below (up) that value, $P < (>) P'$.

Fig. 5

Fig. 5 shows that $P(P')$ increases from 0 ($\cos^2 \alpha (1 + A) / (\cos \alpha + \sqrt{A})^2$) to $(1 + A) / (1 + \sqrt{A})^2$ with increasing β from 0 to α . As $A \leq 1$, P is always less than P' for any β and $|\Phi(\alpha)\rangle$ is used. For $A > 1$, $|\Phi(\beta)\rangle$ is used for β beyond certain value.

The using of the linear optical devices ((polarization) beam splitter, half wave plate, quarter wave plate) and single-mode optical fiber have been demonstrated in the previous experiments. The single-photon one-order M-Z interferometers are used to construct the VBS and the entanglement transformation in each path, and the setup

is equivalent to the two-photon interferometer [3,5,6]. Therefore the scheme is feasible in experiment within current optical technology.

In conclusion, we have described an experimental feasible scheme for producing an arbitrary polarization-entangled mixed state of two photons starting from a pure polarization entanglement with location decoherence. For the entanglement having the special form $\rho = p |\psi\rangle \langle \psi| + (1 - p) |\phi\rangle \langle \phi|$, we also provided a simplified scheme. We believe it should provide a useful source in the exploration of various quantum information processing.

- [1] W. H. Zurek, Phys. Today **44**, 36 (1991).
- [2] C. H. Bennett and D. P. DiVincenzo, Nature **424**, 247 (2000).
- [3] P. G. Kwiat *et al.*, Science **290**, 498 (2000); A. J. Berglund, quant-ph/0010001.
- [4] P. G. Kwiat *et al.*, Phys. Rev. Lett. **75**, 4337 (1995); Phys. Rev. A **60**, 773(R) (1999).
- [5] A. G. White *et al.*, Phys. Rev. Lett. **83**, 3103 (1999).
- [6] P. G. Kwiat *et al.*, Nature **409**, 1014 (2001).
- [7] J.-W. Pan, *et al.*, Nature **410**, 1067 (2001).
- [8] C.-W. Zhang, quant-ph/0104054.
- [9] R. Cleve *et al.*, Phys. Rev. Lett. **82**, 648 (1999).
- [10] C.-W. Zhang *et al.*, Phys. Rev. A **62**, 042302 (2000).
- [11] W. Tittel *et al.*, Phys. Rev. Lett. **81**, 3563 (1998).
- [12] W. K. Wootters, Phys. Rev. Lett. **80**, 2245 (1998).
- [13] M. A. Nielsen, Phys. Rev. Lett. **83**, 436 (1999).
- [14] M. Reck *et al.*, Phys. Rev. Lett. **73**, 58 (1994).
- [15] G. Vidal, Phys. Rev. Lett. **83**, 1046 (1999).

Figure Captions:

Fig. 1. Experimental set-up for preparing an arbitrary polarization-entangled mixed states of two photons.

Fig. 2. Experimental set-up used to generate the mixed states $\rho = p |\psi\rangle \langle \psi| + (1 - p) |\phi\rangle \langle \phi|$.

Fig. 3. The final successful probabilities P (a), P' (b) versus transmission coefficient η_1 . The transformation probabilities $k_1 = 0.8$, $k_2 = 0.7$. Here Solid line, Dot line, and Dash line correspond to the ratio $A = 10000$, 1 , 0.0001 , respectively.

Fig. 4. The final successful probabilities P (solid), P' (dash) versus the ratio A . The transformation probabilities k_1 , k_2 are same as those in Fig. 3.

Fig. 5. The final successful probabilities P , P' versus the angle β . Here $\alpha = 0.7$, $A = 0.001$ in (a) and 1000 in (b).

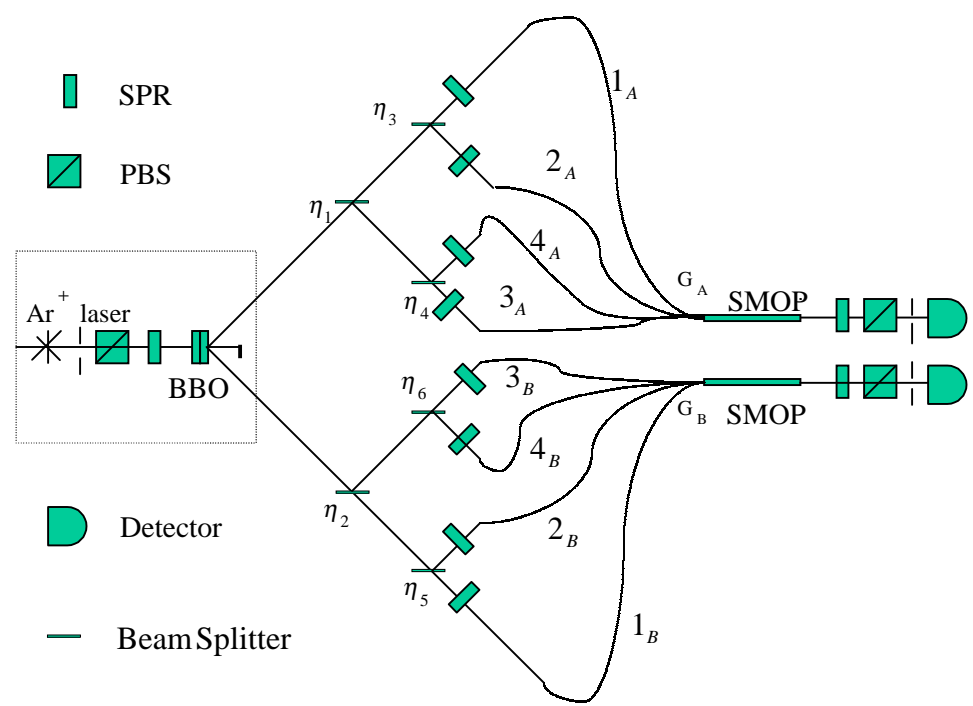


Fig. 1

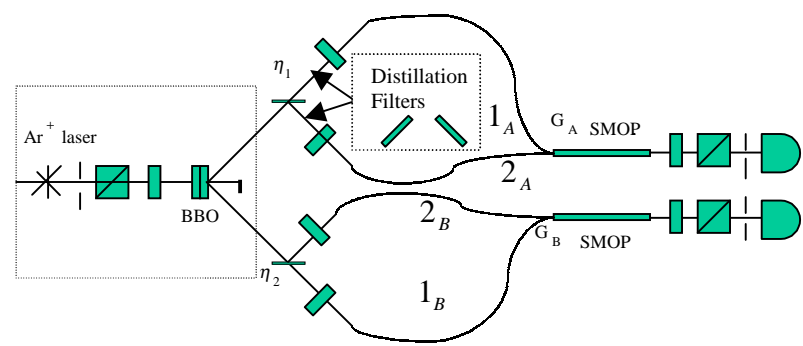


Fig. 2

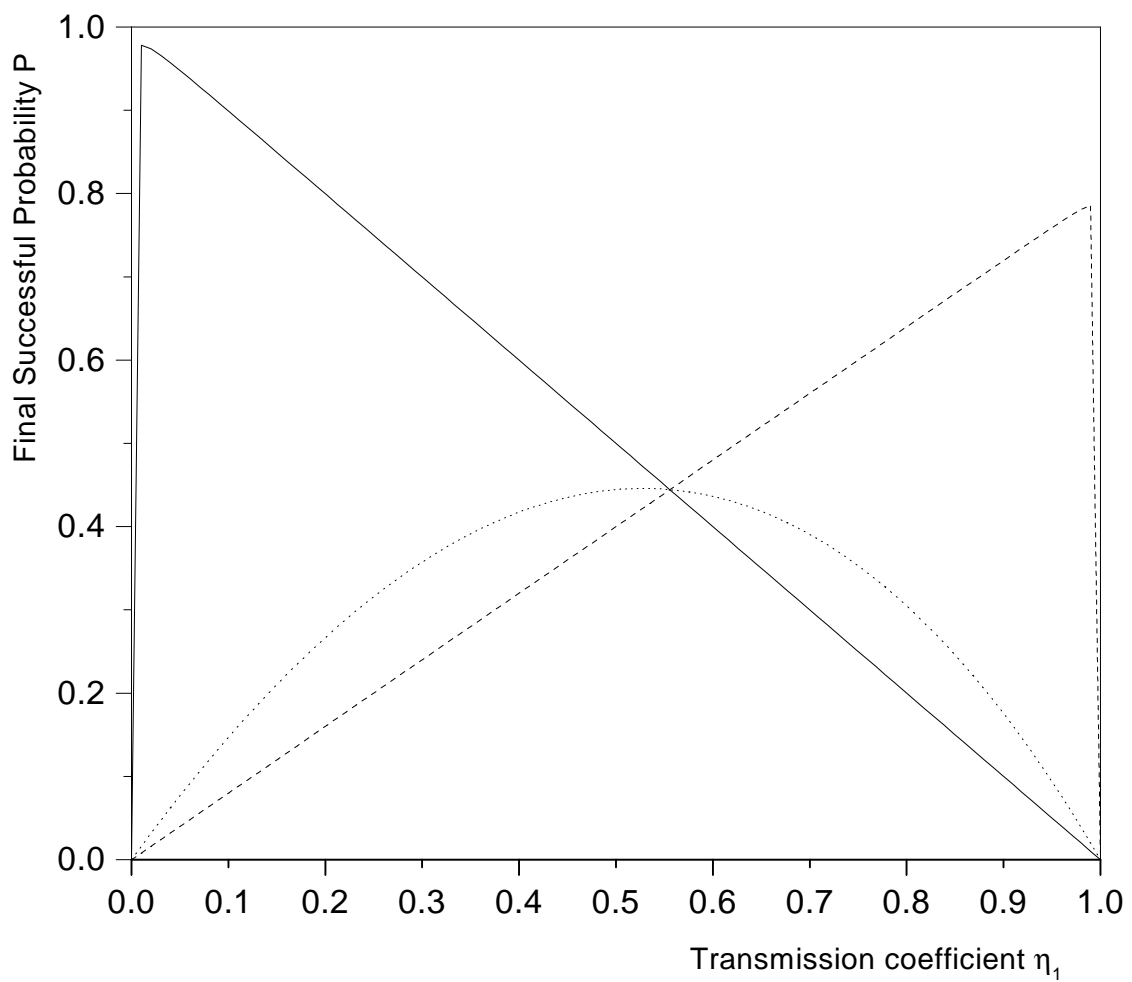


Fig. 3 (a)

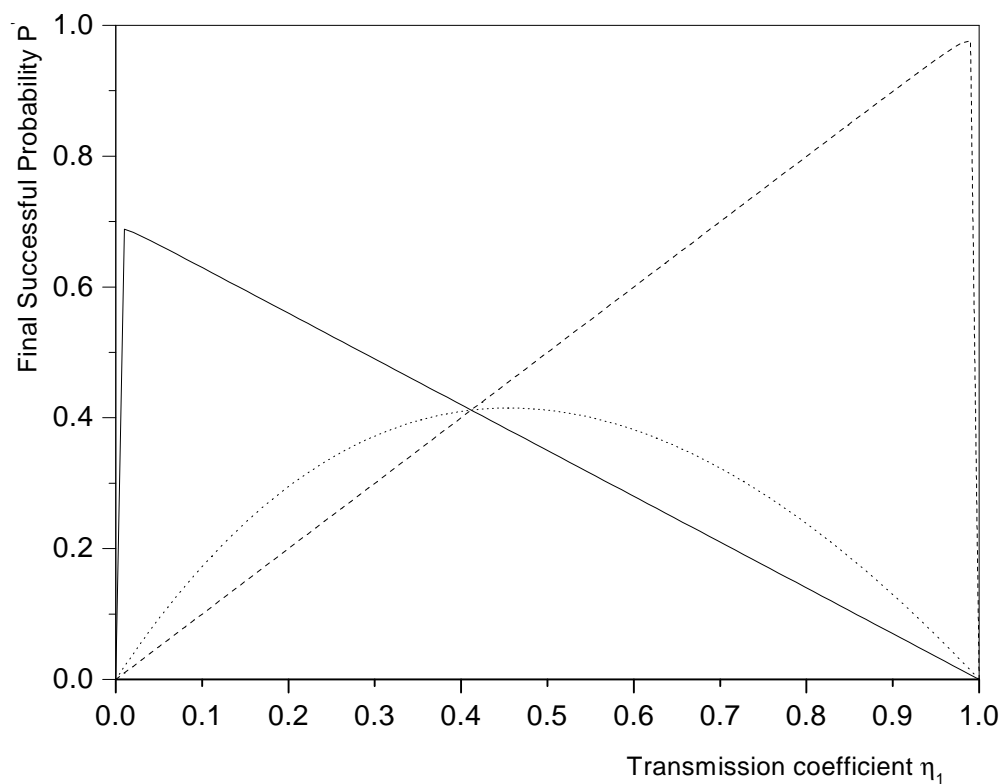


Fig. 3 (b)

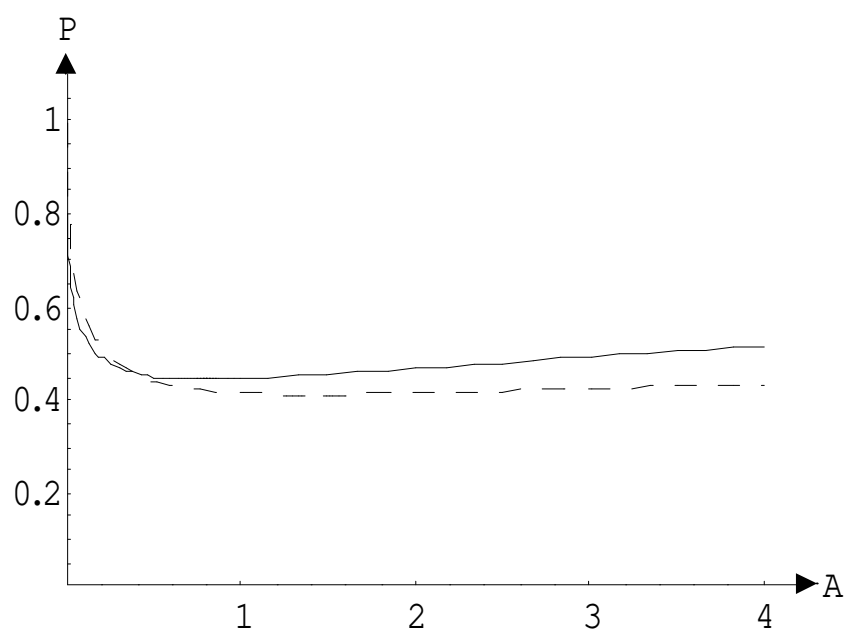


Fig. 4(a)

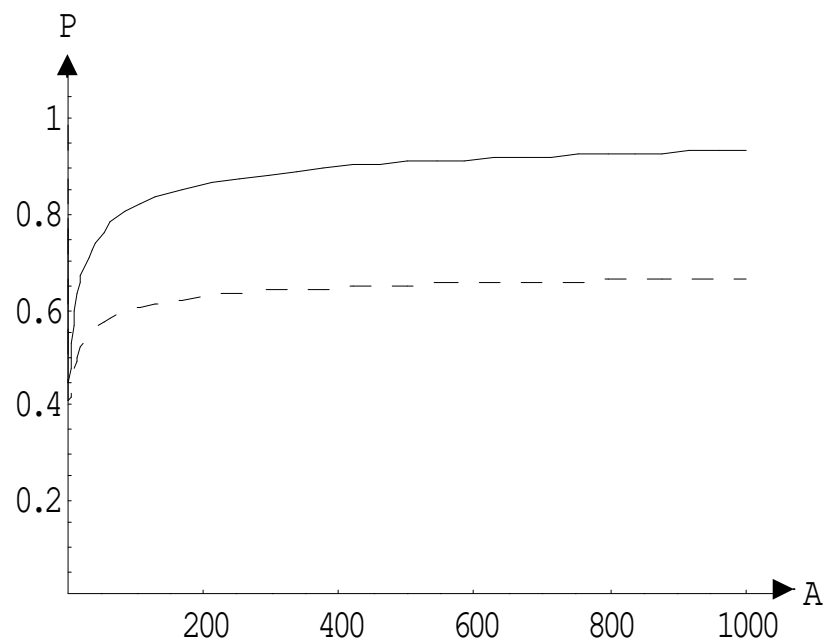


Fig. 4(b)

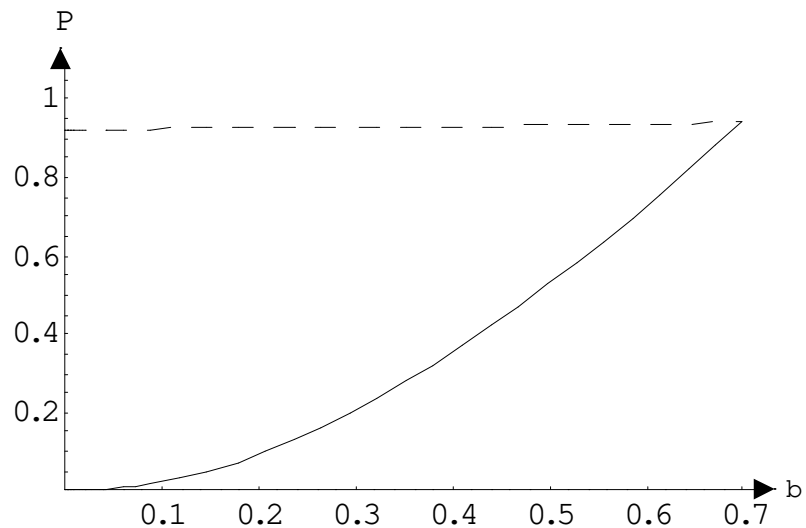


Fig. 5(a)

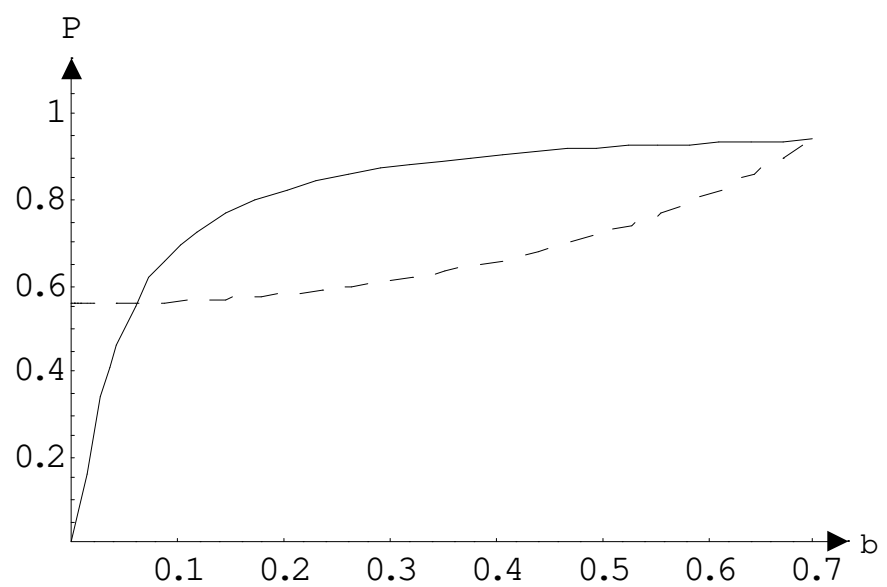


Fig. 5(b)